Adsorption of Methylene Blue from Aqueous Solution using Locust Bean Gum graft Copolymer-Bentonite Composite.

Sirajo Abubakar Zauro[1,2]*, Vishalakshi Badalamoole[1] and Haruna Shehu Ahmed[3]

1. Department of Post-Graduate Studies and Research in Chemistry, Mangalore University, Mangalagangothri, Karnataka, India
2. Department of Pure and Applied Chemistry Usmanu Danfodiyo University, Sokoto, Nigeria
3. Nigerian Defence Acaedermy, Kaduna

Email address: *sirajozauro@gmail.com

Abstract

A graft copolymer gel composite made up of locust bean gum (LBG), diallyldimethylammonium chloride (DADMAC), 2-acrylamido-2- methyl-1-propane sulfonic acid (AMPS) and bentonite (BNT) was prepared using methylenebisacrylamide (MBA) as crosslinker via microwave irradiation and characterized using FTIR, FESEM/EDS and XRD techniques. The graft ted copolymer composite was evaluated for its adsorption towards methylene blue (MB) dye. The LBG-g-poly(DADMAC-co-AMPS)/BNT showed a maximum adsorption of 70.89 mg/g compared to 65.09 mg/g showed by LBG-g-poly(DADMAC-co-AMPS). The adsorption data were subjected to two different isotherm models namely; Freundlich and Langmuir and were observed to be explained best by Freundlich model. The adsorption of MB on the graft copolymer gel and the composite is observed to be a second order kinetic process.

Keywords: Adsorption; Bentonite, diallyldimethylammonium chloride, methylene blue, locust bean gum, 2-acrylamido-2-methyl-1-propane sulfonic acid.

1. Introduction

The use of synthetic materials such as dyes for various industrial uses (textile, leather, paper, rubber, plastic, cosmetic etc) have lead to the proportionate discharge of a large quantity of effluent containing non-biodegradable, toxic and carcinogenic colored substances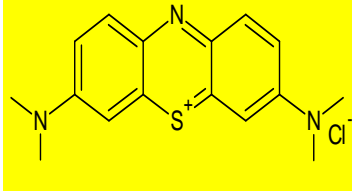 into the environment. This becomes increasingly a major threat to water bodies and the removal of those pollutants from waste water by means of an environmentally friendly technique is a major challenge [1-4].

Methelene blue (MB) is a cationic dye utilise in various field such as Biology, Chemistry, medical sciences and textile industries. The long

Some of the physicacochemical properties of MB are shown in Table 1.

Table 1: Physical properties of methylene blue dye

IUPAC name	3,7-bis(Dimethylamino)-phenothiazin-5-ium chloride
Structure	
Molecular formular	$C_{16}H_{18}ClN_3S$
Molar mass	319.85 g/mol
colour	dark green crystalline powder
Solubility	Soluble in water and ethanol
λ_{max}	663nm

Several techniques such as chemical precipitation, ion exchange, membrane separation, chemical reduction, chemical oxidation, advanced oxidation processes [6] have been employed in the removal of toxic substances from the environment. The efficiency of the above techniques to remove the dye molecules are still low and the methods are time consuming, expensive and sometimes generate large amount of sludge which are toxic to the living organisms in the environment. Hence, adsorption using composite based biopolymers

has been described as one of the most effective and promising technique for removal of such pollutants [7-9].

Locust bean gum (LBG) is a polysaccharide of high molecular weight that is extracted from the seed of carob tree *Ceratoniasiliqua* [10]. LBG consist of a β-1−4-D-mannose chain substituted at the 6 position on varying degree with single α-linked D-galactose residues [11]. It consists mainly of galactose and mannose in 1:4 ratio and is largely known as glactomannose. It has a range of molecular weight between 3×10^5 to 1.2×10^6 DA. It is non ionic, hence its properties unaffected by pH changes within the range of 3-11 or ionic strength [12]. LBG has wide range of applications in fields such as drug delivery [13], water sorption [14], emulsification and gelation [15] etc.

The polymer-clay composite have been gaining increased attention by researchers globally due to the hybrid properties they exhibit when compared with either the polymer or clay separately. A wide range of polymer-clay composite has been produced and used for water treatment [16, 17], dye adsorption [18, 19] etc.

The synthesis of ionic copolymers has been gaining significant interest among researchers [20]. Diallyldimethylammonium chloride (DADMAC) is one of the water soluble cationic monomer that has wide range of applications in water treatment, medicine, etc. [21, 22]. Similarly, 2-acrylamido-2-methyl-1-propane

sulfonic acid sodium salt (AMPS) as an anionic monomer has received attention due to its strongly ionizable sulfonate group [23].

Biopolymers functionalized with ionic monomers with DMDMAC and AMPS can be potential adsorbents for removal of ionic dyes from effluents. Methylene blue is one of the most widely used synthetic dyes in fiber industries for dyeing wool and silk. Despite its potential applications in the textile and leather industries, the MB dye is considered as potent carcinogen, recalcitrant and toxic to mammalian cells [24].

Zhou et al., [25], synthesized a cellulose-graft-poly(acrylic acid) hydrogels via free radical polymerization in phosphoric acid solution and evaluated its capacity towards adsorption of MB from aqueous solution. The results showed that the graft polymer posses an excellent affinity towards MB with maximum adsorption capacity of 2197 mg/g.

Ghorai et. al., [26], reported the synthesis of xanthan gum-graft-polyacrylamide-nanosilica composite for the adsorption of methylene blue and methyl violet. The results showed a remarkable higher adsorption of 99.4% and 99.1% efficiency for MB and MV respectively.

The use of lignocellulose-g-poly(acrylic acid)/montmorillonite composite gel for the removal of MB from aqueous solution was reported [27]. The results showed that the

maximum adsorption capacity for MB on the composite gel is 1994.38 mg/g. The desorption studies revealed that the composite provided the potential for regeneration and reuse after MB dye adsorption, which implied that the composite could be regarded as a potential adsorbent for cationic dye MB removal in a wastewater treatment process.

The adsorption of MB on sodium alginate-graft-polyacrylamide was reported [28]. The adsorption was observed to be pH dependent with maximum adsorption capacity of 69.13 mg/g recorded at pH 10.

Biopolymers functionalised with ionic monomers such as DADMAC and AMPS can be potential adsorbents for ionic dye from aqueous solution. Hence it was planned to develop a copolymer composite gel of DADMAC and AMPS grafted on LBG and its BNT composite for the removal of MB from aqueous solution.

2. Materials and Methods

2.1. Materials

Locust bean gum (LBG), Diallyldimethylammonium chloride (DADMAC), 2-acrylamido-2-methyl propane sulfonic acid (AMPS) were purchased from Sigma Aldrich Chemical Company, India, Ammonium peroxodisulphate (APS) and N, N-methylene-bisacrylamide (MBA) were obtained from SpectroChem Pvt. Ltd Mumbai, India. Methylene blue (MB) was obtained from s. d. fine chemicals Ltd. Mumbai, India. Acetone was

3

obtained from Nice Chemicals pvt Ltd., Kerala, India. Methanol was obtained from Himedia Laboratories Pvt, Ltd., Mumbai, India. All the reagents were used as obtained. Throughout the experiments distilled water was used.

2.2. Methods

2.2.1. Preparation of LBG-g-poly(DADMAC-co-AMPS) gel

The grafting of poly(DADMAC-co-AMPS) on to LBG was carried out as follows; A fixed amount of LBG (0.1g) was dispersed in 20 mL distilled water and stirred overnight followed by addition of APS (0.008) and stirred for an hour. Specified amount of DADMAC (0.15-0.40g) and AMPS (0.1-0.30g) were added to the above solutions followed by MBA (0.005g) and stirred for 8 hours Nie et al, [29]. The solution was then irradiated in a domestic microwave (LG-Gril-Intellowave, India) at 80 watt for 120 seconds with alternate heating and cooling. The solution was then left overnight at ambient temperature to complete grafting and precipitated out using acetone. The precipitate was separated and washed with methanol 2-3 times to remove the un-reacted monomers. The grafted gel was dried in a hot air oven overnight at 50^0C.

2.2.2. Preparation of LBG-g-poly(DADMAC-co-AMPS) gel/BNT

The LBG-g-poly(DADMAC-co-AMPS)/BNT composite gel was made following same procedure as in 2.2.1 above but with addition of BNT under continuous stirring after addition of monomers but prior to microwave irradiation.

2.3. Characterization

LBG, Poly(DADMAC-co-AMPS), LBG-g-poly(DADMAC-co-AMPS) and LBG-gpoly(DADMAC-co-AMPS)/BNT were characterized using standard techniques. The FTIR spectra were recorded in the wave number range of 4000 to 400 cm−1 during 40 scans, with resolution of 2 cm^{-1} using FTIR (Prestige-21, Shimadzu, Japan). The FESEM images were recorded after gold sputtering of the samples in order to make them electrically conductive and scanned at 20 KVA using and JEOL JSM-6380LA (USA) scanning electron microscope. The EDS anysis was carried out using the same FESEM. X-ray diffractograms of the samples were recorded on a bench top X-ray diffractometer, Shimadzu XRD-6000 instrument (Japan). The diffraction patterns was recorded over a 2θ range of 0–80° with a resolution of 0.02° Cu Kα radiation (λ = 1.5406 Å, 30 kV, 30 mA) at room temperature at an analysis rate of 2°/min.

2.4 Dye adsorption study

The adsorption study was carried out in a solution of 100 mg/L of MB solution with known amount of LBG-g-poly(DADMAC-co-AMPS) and LBG-g-poly(DADMAC-co-AMPS)/BNT. The gel and composite samples were immersed in the dye solution and at different time interval 1mL of the solution was withdrawn and diluted appropriately and the

absorbance was measured using UV-visible spectrophotometer (UV-1800 SHIMADZU, Japan) at λmax of 610 nm. Predetermined calibration curves were used to convert the absorbance values into concentration. Equilibrium adsorption studies were also carried out using different dye concentrations (10-100 mg/L). The amount of dye adsorbed at time t and at equilibrium was calculated from the following equations [30].

$$q_t = \frac{(C_o - C_t) \times V}{M}$$

$$q_e = \frac{(C_o - C_e) \times V}{M}$$

Where qt and qe are the amount of MB adsorbed (mg/g) at time t = t and at equilibrium respectively. C0, Ct and Ce are dye concentrations (mg/L) at time t = 0, t = t and at equilibrium respectively. M is the weight of the samples (g) and v is the volume (L) of the MB solution used for adsorption.

3. Results and Discussion

3.1. Preparation of LBG-g-poly(DADMAC-co-AMPS)

The initiator APS under microwave heating generates sulphate anion radicals that attack the LBG and abstract the hydrogen radicals thereby creating reactive sites on LBG molecules (macroradicals). During the polymerisation process, grafting of the copolymer consisting of repeating units of AMPS and DADMAC occurs on LBG macroradicals. The presence of the bi-functional MBA in the copolymer chain results in formation of a gel network of LBG-g-poly(DADMAC-co-AMPS). The presence of inorganic BNT during the polymerisation process which act as fillers leads to the formation of clay entrapped LBG-*g*-poly(DADMAC-*co*-AMPS)/BNT gel composite. The general reaction mechanism for the formation of LBG-g-poly(DADMAC-co-AMPS) in the presence of APS and MBA is shown in Scheme 1.
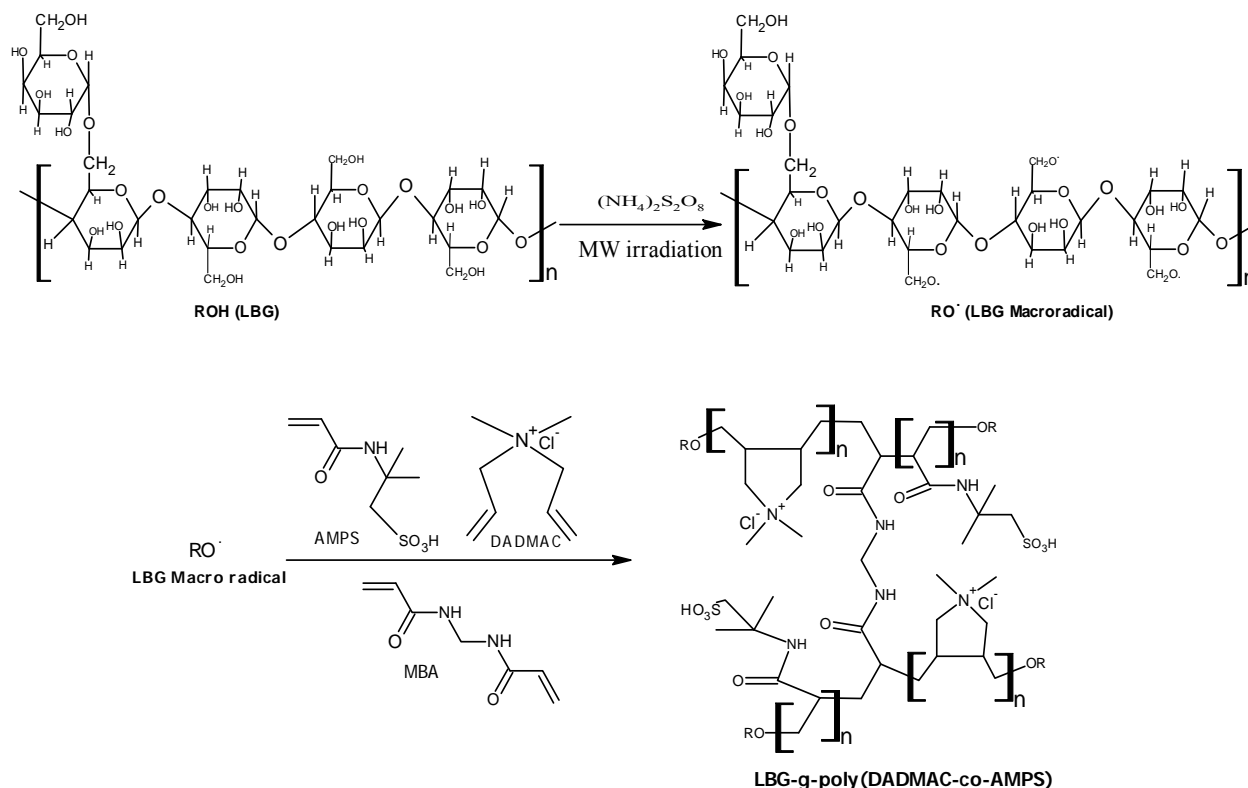
Scheme 1: Proposed scheme for the formation of LBG-g-poly(DADMA-co-AMPS)

3.2. Characterization

3.2.1. FTIR Spectroscopy

The FTIR spectra of LBG, poly(DADMAC-co-AMPS), LBG-g-poly(DADMAC-co-AMPS) and LBG-g-poly(DADMAC-co-AMPS)/BNT are presented in Figure 1. The LBG spectrum (Figure 1a) showed a broad band at 3350 cm^{-1} which is attributed to O-H stretching. The band at 2910 cm^{-1} is assign to C-H$_2$ bending/wagging vibration [31]. The band observed at 1010 cm^{-1} is due to C-O-H stretching. The spectrum of poly(DADMAC-co-AMPS) (Figure 1b) shows an –N-H stretching band at 3426 cm^{-1}, C-H stretching at 2913 cm^{-1}, C-N stretching around 1474 cm^{-1}, C=O stretching of amide at 1615 cm^{-1}, a weak band at 650cm^{-1} due to S-O stretching vibration. For LBG-g-poly(DADMAC-co-AMPS) (Figure 1c), in addition to the bands observed in Figure 3.1a, bands at 1535 cm^{-1} and 1720 were observed due to N-H bending and C=O stretching respectively. In the spectrum of LBG-g-poly(DADMAC-co-AMPS)/BNT shown in Figure 1d, there is a shift in C=O stretching vibration from 1720 to 1649 cm^{-1} and additional occurrence of new bands at 1017, 939 and 808 cm^{-1} for Si-O-Si stretching, Si-O-Al bending and Si-O-C stretching respectively which provides evidence for incorporating BNT into the system.
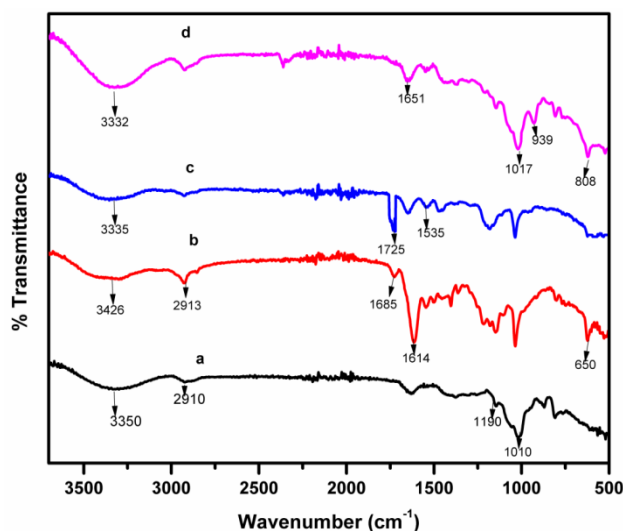
Figure 1: FTIR spectra of; **a)** LBG, **b)** poly(DADMAC-co-AMPS), **c)** LBG-g-poly(DADMAC-co-AMPS) and **d)** LBG-g-poly(DADMAC-co-AMPS)/BNT.

3.2.2. FESEM Analysis

The surface morphology of LBG, poly(DADMAC-co-AMPS), LBG-g-poly(DADMAC-co-AMPS) and LBG-g-poly(DADMAC-co-AMPS)/BNT samples are presented in Figure 2. The smooth, porous and inhomogeneous surface structure of LBG (Figure 2a) undergoes significant change on gel formation. The poly(DADMAC-co-AMPS) shows smooth surface (Figure 2b) compared to LBG. The LBG-g-poly(DADMAC-co-AMPS) (Figure 2c) surface appears cotton-like and irregular. The incorporation of BNT into the system(Figure 2d) produces a coarse and undulant surface with higher porosity compared to LBG-g-poly(DADMAC-co-AMPS).
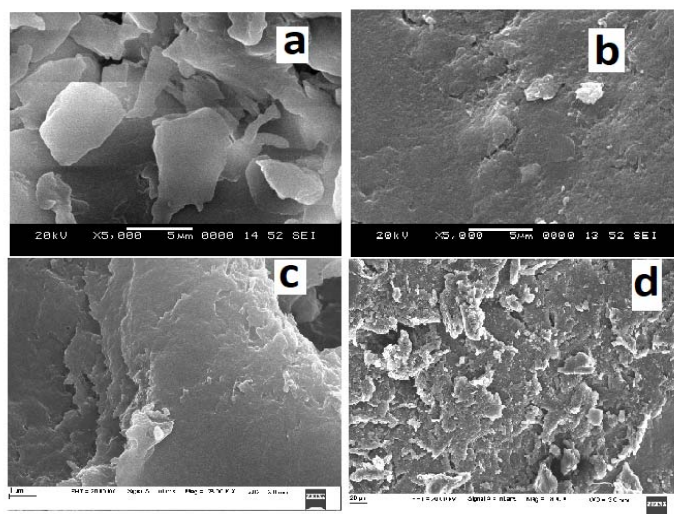

Figure 2: FESEM images of; a) LBG, b) Poly(DADMAC-co-AMPS), c) LBG-g-poly(DADMAC-co-AMPS) and d) LBG-g-poly(DADMAC-co-AMPS)/BNT

7

3.2.3. EDS

The composition of LBG-g-poly(DADMAC-co-AMPS)/BNT was investigated using EDS and the EDS spectrogram (Figure 3) shows elemental distribution over the surface of LBG-g-poly(DADMAC-co-AMPS)/BNT. The presence of Al, Si, Fe and Na peaks in addition to C, N, O and Cl confirmed the incorporation of BNT within the graft copolymer.
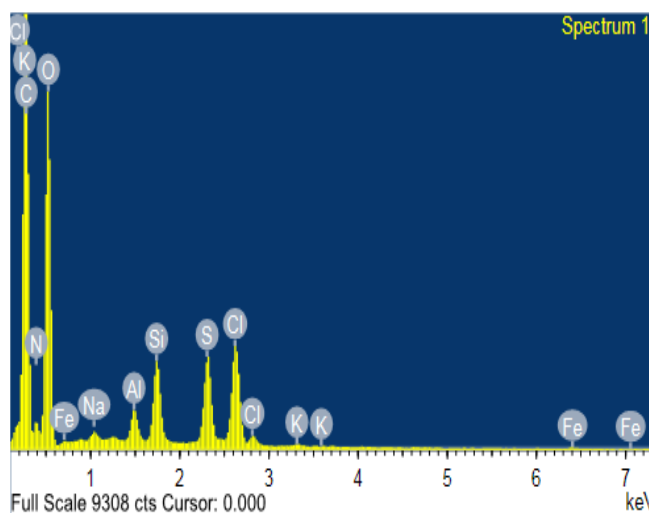

Figure 3: EDS image of LBG-g-poly(DADMAC-co-AMPS)/BNT

3.2.4. XRD

The XRD patterns of LBG, BNT, LBG-g-poly(DADMAC-co-AMPS) and LBG-g-poly(DADMAC-co-AMPS)/BNT are shown in Figure 4. The LBG shows no considerable peak of crystalinity (Figure 4a), hence proved its amorphous nature as reported by [32]. The difractogram of BNT (Figure 4b) shows the crystalline peaks at 2Θ values of 19.76^0, 26.5^0, 34^0 and 62^0. Figure 4c shows clearly that LBG-g-poly(DADMAC-co-AMPS) is amorphous as no crystalline peak is observed in diffractogram. The degree of incorporation of BNT within the graft copolymer (Figure 4d) shows clearly that the highest crystalline peaks ($2\Theta=26.5^0$ and 62^0) that are present in the pure LBG has diminished in the LBG-g-poly(DADMAC-co-AMPS)/BNT. This clearly showed that BNT has been incorporated within the graft-copolymer network.
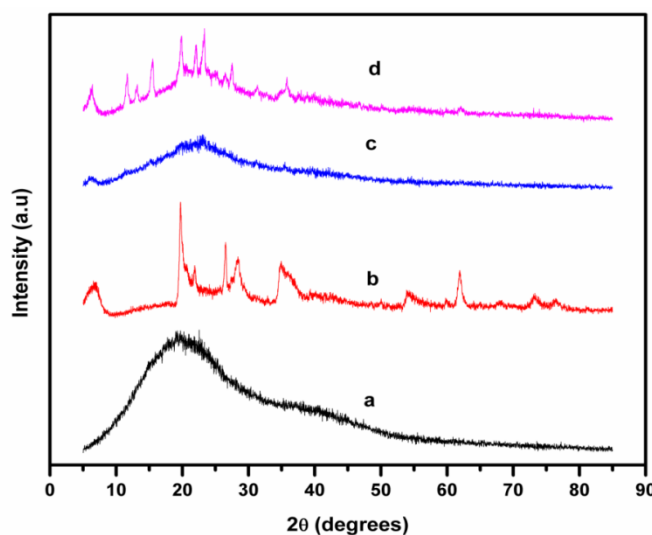
Figure 4: XRD images of; **a)** LBG, **b)** BNT, **c)** LBG-g-poly(DADMAC-co-AMPS) and **d)** LBG-g-poly(DADMAC-co-AMPS)/BNT

3.3. Adsorption of MB

The adsorption studies was carried out using MB as model dye.

> **Effect of contact time**

The effect of contact time on the adsorption capacity of LBG-g-poly(DADMAC-co-AMPS) and LBG-g-poly(DADMAC-co-AMPS)/BNT towards MB is shown on Figure 5. Initially, the adsorption on both adsorbents proceeded slowly up to 30 minutes and gradually 420 minutes for the LBG-g-poly(DADMAC-co-AMPS)/BNT and 180 minutes for LBG-g-poly(DADMAC-co-AMPS). Fast adsorption was observed between 420 to 540 minutes on all the adsorbents. The adsorption of equilibrium was reached between 540 to 600 minutes. The equilibrium adsorption capacity for MB was found to 65.09 and 70.89 mg/g respectively for LBG-g-poly(DADMAC-co-AMPS) and LBG-g-poly(DADMAC-co-AMPS)/BNT. The adsorption of MB is attributed to the electrostatic interaction between the adsorbents and the asorbates. The higher adsorption by LBG-g-poly(DADMAC-co-AMPS)/BNT compared to LBG-g-poly(DADMAC-co-AMPS) is attributed to H-bonding interactions as well as dipole−dipole and electrostatic interactions between anionic site of BNT and cationic site of MB molecules [26].
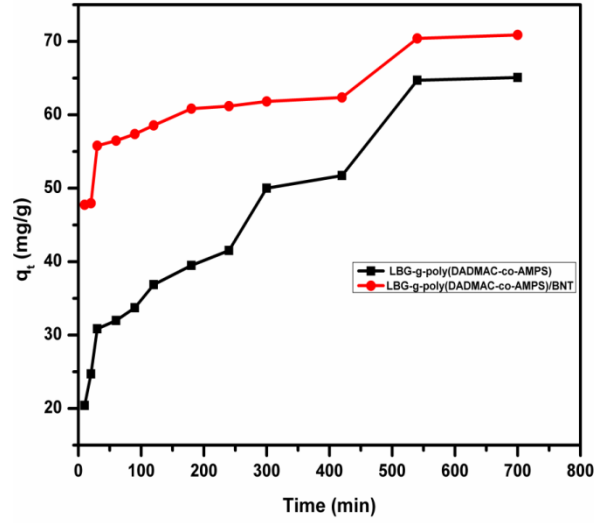
9

Figure 5: Effect of contact time on the adsorption of MB on the adsorbents (adsorbent dose=120 mg; C_0 = 100 mg/L; V=100 mL and pH 7.0)

3.3.1 Adsorption kinetics

The kinetics study for the adsorption of MB was investigated using the two most commonly used kinetic models. The are;

> **Lagergren Pseudo First Order Kinetics**

The pseudo first order kinetic model is expressed by the linear relationship [33] by the following equation.

$$\log(q_e - q_t) = log q_e - \frac{K_1}{2.303} t$$

Where q_e and q_t are the amount of MB (mg/g) adsorbed at equilibrium and at time t respectively, k_1 is the rate constant (min^{-1}) for the pseudo-first order kinetics and t is the time (min.). The rate constant (k_1) and correlation coefficient were calculate from the plot of *log* *(q_e-q_t) vs t* (Figure 6) and tabulated in Table 1. It was observed from the data presented in Table 1 that there is no aggrement between the $q_{e\ (cal)}$ and $q_{e\ (exp)}$. Also, the R^2 values are low in all cases, hence adsorption of MB onto LBG-g-poly(DADMAC-co-AMPS) and LBG-g-poly(DADMAC-co-AMPS)/BNT cannot be well explain by the pseudo-first order kinetic model.
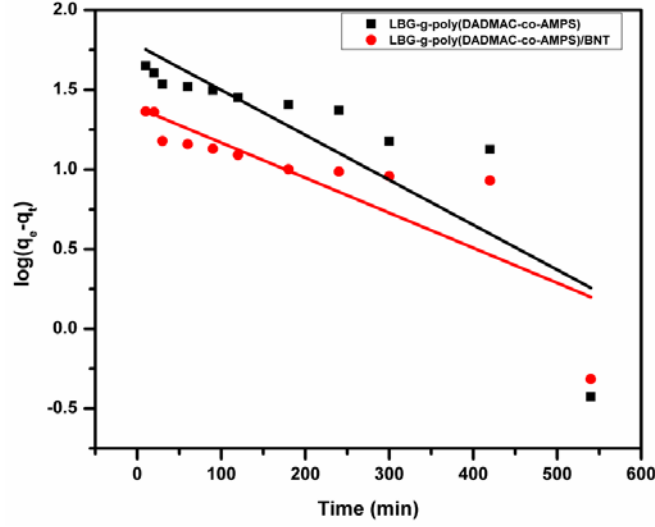
10

Figure 6: Pseudo fisrt order kinetic for the adsorption of MB the adsorbents

➢ Pseudo Second Order Kinetics

The linear form of pseudo second order kinetic equation [34] is represented by the following equation;

$$\frac{t}{q_t} = \frac{1}{k_2 q_e^2} + \frac{1}{q_e} t$$

Where q_e and q_t are as defined earlier, k_2 is the second order rate constant (g/mg/min). The plot of t/q_e vs t (Figure 7) gives a straight line from which it can be concluded that the adsorption of MB is well explained by pseudo second order

kinetic process. This indicated that adsorption's mechanism is chemically rate controlling (chemisorptions). The values of q_e, k_2 and R^2 obtained from the intercept and slope of t/q_t vs t plots (Figure 7) are presented in Table 1. The R^2 values are 0.957 and 0.953 respectively on LBG-g-poly(DADMAC-co-AMPS) and LBG-g-poly(DADMAC-co-AMPS)/BNT. Furthermore, the values of $q_{e\ (cal)}$ obtained from pseudo second order are in good agreement with the $q_{e\ (exp)}$ compared to pseudo first order kinetic model.
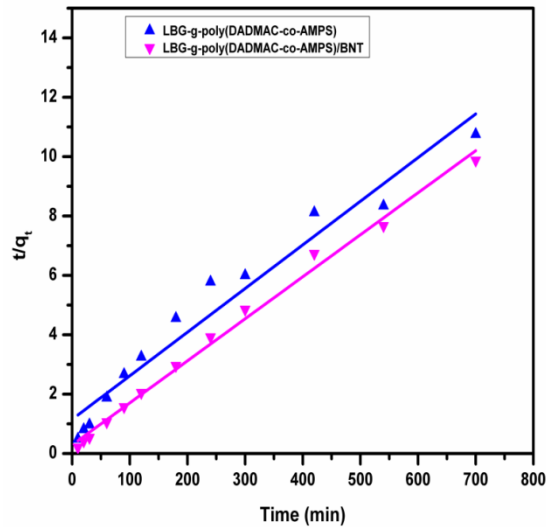

11

Figure 7: Pseudo second order kinetic for the adsorption of MB onto adsorbents

Table 1: Kinetics data for the adsorption of MB

	Parameters	LBG-g-poly(DADMAC-co-AMPS)	LBG-g-poly(DADMAC-co-AMPS)/BNT
First	$q_{e\ exp.}$ (mg/g)	65.09	70.89
	q_{ecal}(mg/g)	60.26	24.43
	k_1 (min^{-1})	0.006	0.005
	R^2	0.719	0.717
	q_{ecal}(mg/g)	71.43	71.43
	k_2 (g/g$^/$min)	0.002	0.0007
Second	R^2	0.957	0.993

3.3.2. Adsorption Isotherms

For equilibrium adsorption studies, fixed amount (0.05g) of the adsorbents were used in 25mL solution containing varied concentration of MB (10-100 mg/L) and the maximum amount of MB adsorbed in each case was determined. The two isotherm models namely; Freundlich [35] and Langmuir [36] were employed in this work in order to understand the adsorption behavior of the dyes on the adsorbents.

> **Freundlich Isotherm**

The Freundlich isotherm model assumes multilayer adsorption. It is based on the assumption that encompasses the heterogeneity of the surface and the adsorption capacity is related to the equilibrium concentration of the adsorbate. The Freundlich isotherm is commonly expressed as;

$$\ln q_e = lnk_f + \frac{1}{n}lnC_e$$

Where q_e and C_e are the amount of MBadsorbed (mg/g) and the equilibrium concentration of MB (mg/L) respectively, k_f (mg/g) and n are Freundlich adsorption isotherm constants that represent the adsorption capacity of MB and the degree of nonlinearity between the MB concentration and the adsorbents respectively.The values of k_f and n were calculated from the intercept and slope of the plot of *log q_e vs log C_e* (Figure 8) and are presented in Table 2. The adsorption of MB on LBG-g-poly(DADMAC-co-AMPS) and LBG-g-poly(DADMAC-co-AMPS)/BNT is considered to be favourable (n=1-10). Similarly, the value of R^2 in all cases are higher and move towards unity which is an indication of the fitting of adsorption data into the model.

The value of k_f obtained from both adsorbents are low compared to 2.51 mg/g obtained by Pathania *et al,* [5] for activated carbon, 75.2 mg/g by El Moouzdahir *et al*, [37] on Moroccan

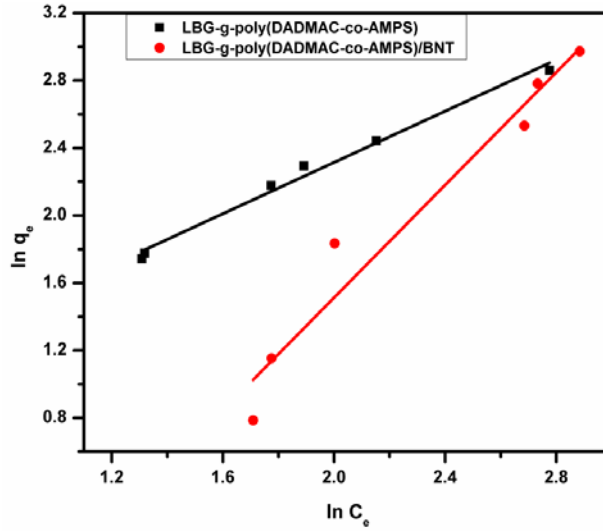clay and 13.6 mg/g by Yao *et al*, [38] on cabon   nanotubes.

Figure 8: Freundlich isotherm for MB onto the adsorbents

> ➤ **Langmuir Model**

The Langmuir isotherm is a model which quantitatively describes formation of the equilibrium monolayer of adsorbate molecules on the surface of the adsorbent and is expressed as follows;

$$\frac{C_e}{q_e} = \frac{1}{q_m} \cdot C_e + \frac{1}{K_L\,q_m}$$

where, C_e and q_e are as defined earlier, q_m is the maximum adsorption corresponding to complete monolayer coverage on the surface (mg/g) and K_L is the Langmuir constant which is related to the energy of adsorption (L/mg). K_L and q_m are determined from the intercept and slope of the linear plot of C_e/q_e vs C_e (Figure 9). The essential feature of the Langmuir isotherm can be represented in terms of separation factor (dimensionless equilibrium parameter) R_L [39], which can be expressed as;

$$R_L = \frac{1}{1 + K_L C_o}$$

where, C_0 is the initial concentrations of MB, K_L is the constant related to the energy of adsorption (Langmuir Constant). R_L value indicates the favorability of adsorption. If $R_L > 1$ the adsorption is unfavorable, if $R_L = 1$ the adsorption is linear, if $0 < R_L < 1$ the adsorption is favorable and if $R_L = 0$ then the adsorption is irreversible.

The Langmuir isotherm data are presented in Table 2. The R_L values obtained in this study showed favorable adsorption of MB on the gel.

The maximum adsorption capacity (q_m) of 43.38 and 10.75 mg/g on the gel and composite respectively are low compared to values obtained by Pathania *et al,* [5] (47.62 mg/g) for activated carbon, Elmoouzdahir *et al,* [37] (142 mg/g) on Moroccan clay and Yao *et al.,* [38] (35.4 mg/g) on cabon nanotubes.
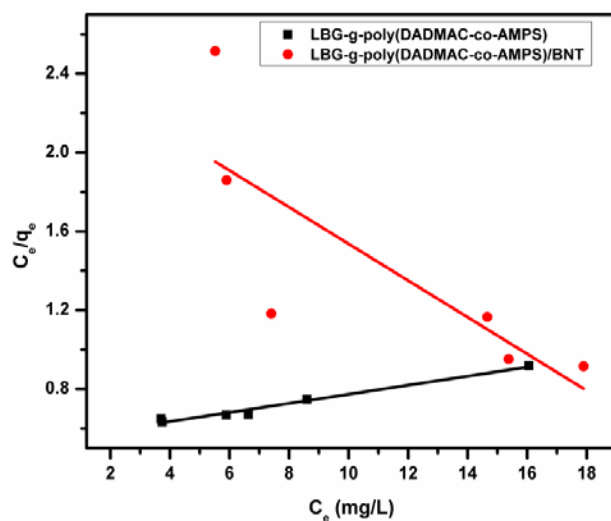
Figure 9: Langmuir isotherm for MB onto the adsorbents

Table 2: Adsorption isotherms data for MB

	Parameters	LBG-g-poly(DADMAC-co-AMPS)	LBG-g-poly(DADMAC-co-AMPS)/BNT
Freundlich	n	1.32	0.60
	k_f(mg/g)	2.21	0.16
	R^2	0.989	0.956
Langmuir	q_{max}(mg/g)	43.48	10.75
	R_L	0.70	1.60
	k_L(L/mg)	0.042	0.04
	R^2	0.978	0.648

3.3.3. Desorption studies

One of the most important features of adsorbent is its regeneration ability. This is because it simplifies the sewage treatment manipulation, save cost and increase the disposal efficiency of

.

dye wastewater [40]. Figure 10 showed the percentage desorption of MB in acidic and alkaline medium. It was observed that higher amount of MB on the composites was recovered in both acidic and alkaline medium
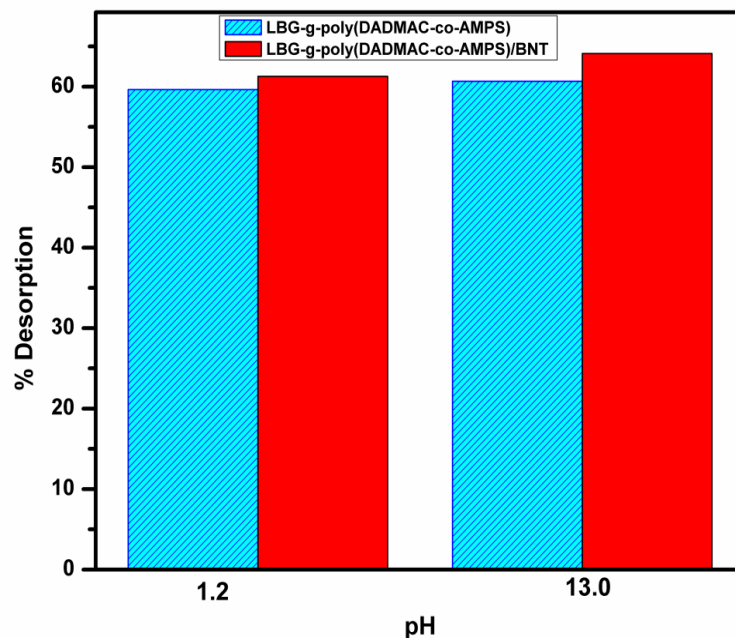
Figure 10: % desorption of the adsorbed MB from the adsorbents

4. Conclusion

In this chapter, a graft-copolymer gel consisting of LBG, DADMAC, AMPS and its composite with BNT clay were made via microwave irradiation. The adsorption of MB on the graft-copolymer gel and the composite revealed that MB was adsorbed more on both LBG-g-poly(DADMAC-co-AMPS)/ BNT than LBG-g-poly(DADMAC-co-AMPS). The adsorption data were observed to fit best into Freundlich model and the adsorption is found to follow second order kinetic model.

References

[1]. Malana, M, A., Ijaz, S. and Ashiqm, M. N. (2010). *Desalination*, **263:** 249-257.

[2]. Zhou, C., Wu, Q., Lei, T and Negulescu, I. I. (2014). *Chem. Eng. J.*, **251:** 17-24.

[3]. Gan, L., Shang, S., Hu, E., Yuen, C. W. M. and Jiang, S. (2015). *Appl. Sur. Sci.*, **357:** 866-872.

[4]. Fosso-kankeu, E., Mittal, H., Mishra, S. B. and Mishra, A. K. (2015). *J. Ind. Eng. Chem.,* **22:** 171.178.

[5]. Pathania, D., Sharma, S. and Singh, P. (2017). *Arab. J. Chem.,* 10(1): S1445-S1451

[6]. Santos, S. C. R., Boaventura, R. A. R. (2016). *J. Environ. Chem. Eng.,* **4:** 1473–1483.

[7]. Mahida, V. P., Patel, M. P.(2016). *Chin. Chem. Lett.*, **27:** 471–474.

[8]. Maity, J., Ray, S. K.(2016). *Int. J. Biol. Macromol.*, **89:** 246-255.

[9]. Robati, D., Mirza, B., Ghazisaeidi, R., Rajabi, M., Moradi, O., Tyagi, I., Agarwal, S., Gupta, V. K. (2016). *J. Mol. Liq.,* **216:** 830–835.

[10]. Kaity, S., Isaac, J., Kumar, P. M., Bose, A., Wong, T. W. and Ghosh, A. (2013). *Carbohydr. Polym., * **98:**1083– 1094

[11]. Kaity, S. and Ghosh, A. (2013). *Ind. Eng. Chem. Res., * **52:** 10033−10045

[12]. Nisperos-Carriedo, M. O. (1994). Edible coatings and films based on polysaccharides. In: Krochta, J. M., Baldwin, E. A., Nisperos-Carriedo, M.O., (eds), Edible films and coatings to improve food quality. Lancaster: Technomic, 305–36.

[13]. Maiti, S., Dey, P., Banik, A., Sa, B., Ray, S. and Kaity, S. (2010). *Drug Del., * **17(5):** 288–300

[14]. Sundaram, J. and Durance, T. D. (2008). *Food Hydrocolloids, * **22:**1352–1361

[15]. Kawamura, Y. (2008). Carob bean gum chemical and technical assessment (CTA) for the 69th JECFA. Page 1-6

[16]. Sebastian, S., Mayadevi, S., Beevi, B. S., Mandal, S. (2014). *J. Water Res. Prot., * **6:** 177-184.

[17]. Gupta, S. K., Nayunigari, M. K., Misra, R., Ansari, F. A., Dionysiou, D. D., Maity, A., Bux, F.(2016). *Ind. Eng. Chem. Res., * **55:** 3−20.

[18]. El Haddad, M., Mamouni, R., Saffaj, N., Lazar, S.(2012). *Glob. J. Hum. Soc. Sci. Geog. & Environ. Geo-Sci., * **12:** 19-29

[19]. Patil, M. R., Shrivastava, V. S. (2015). *J. Mater. Environ. Sci., * **6:** 11-21

[20]. Tirelli, N and Hunkeler, D. J. (1999). *Macromol. Chem. Phys., * **200 (5):** 1068-1073

[21]. Jing, R. and Hongfei, H. (2001). *Eur. Polym. J., * **37:** 2413- 2417.

[22]. Zhao, Q., Sun, J., Chen, S and Zhou, Q. (2010). *J. Appl. Polym. Sci., * **115(5):** 2940-2945.

[23]. Durmaz, S. and Okay, O. (2000). *Polymers*, **41(10):** 3693– 3704.

[24]. Gopi, S., Balakrishnan, P., Piusa, A. and Thomas, S. (2017). *Carbohydr. Polym.*, **165:** 115–122.

[25]. Zhou, Y., Fu, S., Liu, H., Yang, S. and Zhan, H. (2011). *Polym. Eng. Sci., * **51:** 2417-2422

[26]. Ghorai, S., Sarkar, A., Raoufi, M., Panda, A. B., Schö nherr, H.and Pal, S. (2014). *ACS App. Mat. Interfaces*, **6:** 4766−4777

[27]. Shi, Y., Xue, Z., Wang, X., Wang, L. and Wang, A. (2013). *Polym. Bull.*, **70:** 1163–1179

[28]. da Feira, J. M. C., Klein, J. M. and Forte, M. M. D. C. (2018). *Polímeros*, **28(2):** 139-146

[29]. Nie, X., Adalati, A., Du, J., Liu, H., Xu, S. and Wang J (2014). *Appl. Clay Sci.*, **97–98:**132–137

[30]. Karthika, J. S. and Vishalakshi, B. (2015). *Int. J. Biol. Macromol., * 81:544–655

[31]. Kaity, S., Isaac, J., Ghosh, A. (2013). *Carbohydr. Polym., * **94:** 456– 467

[32]. Martins, J. T., Cerguira, M. A., Bourbon, A. I., Pinheiro, A. C., Souza, B. W. S., Vicente, A. A. (2012). *Food Hydrocolloids, * **29(2):** 280-289

[33]. Lagergren, S. (1898). K. Sven. Vetenskapsakad. Handl., *. 24 (4):* 1-39.

[34]. Ho, Y. S. and McKAY, G. (1998). *Trans Ichem E*, **76 Part B:** 332- 340

[35]. Freundlich, H., Heller, W. (1939). *J. Am. Chem. Soc.*, **61(8):** 228-230

[36]. Langmuir, I. (1916). *J. Am. Chem. Soc., * **38 (11):** 2221–2295

[37]. El Mouzdahir, Y., Elmchaouri, A., Mahboub, R., Gil, A. and Korili, S. A. (2007). *J. Chem. Eng. Data, * 52: 1621-1625

[38]. Yao, Y., Xu, F., Chen, M., Xu, Z. and Zhu, Z. (2010). *Bioresour. Technol.,*101(9): 3040-3046

[39]. Krishna, R. H., & Swamy, A. V. (2012). *Int. J. Eng. Res.Dev., 4* **(1):** 29-38.

[40]. Chen, M., Ding, W., Wang, J., Diao, G. (2013). *Ind. Eng. Chem. Res.,* **52(6):** 2403−2411

Authors' contributions

This work was carried out in collaboration between all authors. Author SAZ designed the study, performed the experiments and wrote the first draft of the manuscript. Authors BV gone through entire manuscript for necessary modification and improvements. Author HAS managed the final analyses of the study. All authors read and approved the final manuscript